

1 **Efficient and highly amplified imaging of nucleic acid targets in cellular and**
2 **histopathological samples with pSABER**

3
4 Sahar Attar^{1,2}, Valentino E. Browning¹, Yuzhen Liu¹, Eva K. Nichols¹, Ashley F. Tsue^{4,5,6}, David
5 M. Shechner^{4,5,6}, Jay Shendure^{1,5,6,7,8}, Joshua A. Lieberman², Shreeram Akilesh^{2,3*}, Brian J.
6 Beliveau^{1,5*}

7
8 ¹Department of Genome Sciences, University of Washington, Seattle, WA, USA

9
10 ²Department of Laboratory Medicine and Pathology, University of Washington, Seattle, WA,
11 USA

12
13 ³Kidney Research Institute, Seattle, WA, USA

14
15 ⁴Department of Pharmacology, University of Washington, Seattle, WA, USA

16
17 ⁵Brotman Baty Institute for Precision Medicine, Seattle, WA, USA

18
19 ⁶Institute of Stem Cell and Regenerative Medicine, University of Washington, USA

20
21 ⁷Allen Discovery Center for Cell Lineage Tracing, Seattle, WA, USA

22
23 ⁸Howard Hughes Medical Institute, University of Washington, Seattle, WA, USA

24
25 *Correspondence e-mail: shreeram@uw.edu; beliveau@uw.edu

26
27
28
29
30
31
32
33
34
35
36
37
38
39
40
41
42
43
44
45
46
47
48

1 **Abstract**

2 *In situ* hybridization (ISH) is a powerful tool for investigating the spatial arrangement of nucleic
3 acid targets in fixed samples. ISH is typically visualized using fluorophores to allow high
4 sensitivity and multiplexing or with colorimetric labels to facilitate co-visualization with
5 histopathological stains. Both approaches benefit from signal amplification, which makes
6 target detection effective, rapid, and compatible with a broad range of optical systems. Here,
7 we introduce a unified technical platform, termed 'pSABER', for the amplification of ISH signals
8 in cell and tissue systems. pSABER decorates the *in situ* target with concatemeric binding sites
9 for a horseradish peroxidase-conjugated oligonucleotide which can then catalyze the massive
10 localized deposition of fluorescent or colorimetric substrates. We demonstrate that pSABER
11 effectively labels DNA and RNA targets, works robustly in cultured cells and challenging
12 formalin fixed paraffin embedded (FFPE) specimens. Furthermore, pSABER can achieve 25-
13 fold signal amplification over conventional signal amplification by exchange reaction (SABER)
14 and can be serially multiplexed using solution exchange. Therefore, by linking nucleic acid
15 detection to robust signal amplification capable of diverse readouts, pSABER will have broad
16 utility in research and clinical settings.

17

18

19

20

21

22

23

24

25

26

27

28

29

30

31

32

33

34

35

36

37

38

39

40

41

42

43

44

45

46

47

48

1 **Introduction**

2 Since its introduction by Pardue and Gall¹ in the late 1960s, *in situ* hybridization (ISH)
3 has been widely used in research and clinical settings to determine the abundance and
4 subcellular location of nucleic acid targets. ISH relies on the formation of heteroduplexes
5 between target RNA and DNA strands present in fixed cellular and tissue samples and
6 complementary probe strands that are added during a hybridization reaction. Once completed,
7 the results of the hybridization reaction can be visualized using transmitted light or fluorescent
8 microscopy depending on the type of labeling strategy used. Common applications for ISH
9 include targeting intervals of genomic DNA to assay chromosome copy number in cytogenetic
10 clinics², the quantitative profiling of single-cell RNA expression profiles³, the investigation of
11 how chromosomes are spatially organized within the nucleus⁴, and the visualization of gene
12 expression patterns in whole mount tissue specimens⁵.

13 Considerable technical development has occurred to improve the sensitivity of ISH and
14 to broaden its applications. Among these, notable developments include the transition from
15 radioactive to fluorescent labels^{6–8}, the use of recombinant⁹ and synthetic^{3,10–13} DNA as a source
16 of probe material, and the introduction of massively multiplexed imaging approaches that rely
17 on iterative rounds of hybridization and imaging in the same sample^{14–16}. Another set of
18 technical development has focused on strategies to amplify the signal of ISH, which has
19 particular benefits in challenging sample types such as formalin-fixed, paraffin-embedded
20 (FFPE) tissue sections, thick frozen tissue sections, and whole mount tissue samples^{17,18}.
21 Broadly, these signal amplification approaches fall into two categories: 1) Assembly-based
22 technologies in which DNA and/or protein species are directed to the site(s) of ISH in order to
23 create an *in situ* scaffold capable of recruiting many directly labeled molecules to increase the
24 overall label density at the target site. Examples of assembly-based approaches include the
25 assembly of branched DNA (bDNA)^{19,20} and LNA²¹ structures, hybridization chain reaction
26 (HCR)²², and ClampFISH^{23,24}, 2) Enzymatic approaches in which specialized probe sets recruit
27 enzymes to catalyze the formation signal amplification structures *in situ*. Examples of
28 enzymatic approaches include the catalyzed reporter deposition (CARD) technique that uses
29 the horseradish peroxidase (HRP) enzyme to locally deposit detectable biotin molecules²⁵,
30 methods that recruit HRP or alkaline phosphatase for colorimetric detection via haptene
31 probes in whole-mount embryos²⁶, and rolling circle amplification (RCA)²⁷.

32 Assembly-based and enzymatic signal amplification approaches can strengthen signals
33 by >100x, making it easier to detect analytes in thick and noisy sample types. These methods
34 even make it possible to image labeled specimens on low numerical aperture imaging systems
35 with lower photon collection efficiencies. However, as these approaches require that the signal
36 amplification structure be created *in situ*, they can be difficult to troubleshoot, particularly for
37 researchers who are performing ISH itself for the first time. Moreover, many of these
38 approaches rely on costly or proprietary reagents, which adds to the difficulty of establishment
39 and implementation. The recently developed signal amplification by exchange reaction
40 (SABER) technique introduced by Kishi and colleagues²⁸ abrogates these issues, as signal
41 amplification in SABER is achieved by the *in vitro* addition of long, concatemeric ssDNA tails to
42 the probe molecules via the primer exchange reaction (PER)²⁹ prior to their addition to the fixed
43 sample. As the creation of the signal amplification structure occurs *in vitro*, researchers can
44 evaluate the results of the PER reaction and troubleshoot as needed prior to executing time
45 consuming ISH experiments with precious samples. In addition to this useful feature, SABER
46 has many strong attributes as a signal amplification approach, including low-cost (\$1–5 per
47 sample) simple and robust multiplexing via solution exchange²⁸.

48 While SABER has features that may accelerate its adoption, it still has limitations. For
49 instance, SABER can achieve ~450x signal amplification when it employs iterative rounds of

1 branched assembly *in situ*²⁸, but to date that approach has only been shown for imaging one
2 target at a time and has only been used on cultured cells, and the unbranched form of SABER
3 that supports multicolor imaging in cells and tissues only provides a more modest ~5–15x
4 amplification²⁸. SABER also has yet to be combined with colorimetric detection methods,
5 which facilitate co-visualization with histopathological stains such as hematoxylin and eosin.
6 Here, we introduce ‘peroxidase-SABER’ (pSABER), a robust and cost-effective strategy for
7 boosting the signal of SABER by a further 20-fold and expanding its readout modalities to
8 include colorimetric detection. We demonstrate the effectiveness of colorimetric and
9 fluorescent pSABER in fixed cells and FFPE tissue sections and showcase the ability of
10 pSABER to perform highly amplified and multiplexed imaging via solution exchange. We
11 anticipate that its simplicity and its seamless integration into the existing SABER toolkit will
12 lead to the adoption of pSABER as a workhorse technique for *in situ* nucleic acid detection in
13 research and clinical settings.

14

15

16 **Results**

17

18 **Programming enzymatic signal amplification with pSABER**

19 The pSABER approach builds on the established, unbranched SABER workflow. First,
20 probe sets or “readout oligos” complementary to a common exogenous binding site encoded
21 in complex oligo probe libraries are extended *in vitro* by the primer exchange reaction
22 (PER)^{28,29}, resulting in the addition of long concatemers of a reiterated 10 nt PER sequence (Fig.
23 1). These concatemers are then applied to the sample and primary *in situ* hybridization is
24 performed (and secondary hybridization with extended readout oligos in the case that readout
25 oligos are being used). To detect the hybridized concatemers, the sample is then hybridized
26 with a 20 nt oligo covalently conjugated to HRP that is complementary to a dimer of the
27 reiterated PER sequence (Fig. 1). Finally, the sample is incubated with H₂O₂ and an HRP
28 substrate to facilitate the localized deposition of a variety of colorimetric or fluorescent labels
29 that can be detected by microscopy (Fig. 1).

30

31 **pSABER enables amplified colorimetric detection**

32 In order to validate the pSABER approach and demonstrate its compatibility with
33 colorimetric detection, we designed a series of RNA and DNA ISH experiments against well-
34 established molecular targets. We first performed an RNA ISH experiment using a probe set
35 consisting of 83 oligos targeting the ADAMTS1 mRNA in human K29Mes cells that had been
36 shifted to 37°C prior to fixation to induce ADAMTS1 expression³⁰. After primary hybridization,
37 the sample was developed with 3,3'-Diaminobenzidine (DAB) in the presence of H₂O₂ prior to
38 hematoxylin staining and mounting. Upon visualization by routine brightfield microscopy, both
39 robust cytoplasmic DAB staining consistent with single-molecule RNA FISH³ and strong
40 nuclear puncta corresponding to sites of induced transcription³⁰ were observed, neither of
41 which was visible in the no primary probe negative control (Fig. 2a). To test the applicability of
42 pSABER to more challenging DNA ISH applications, we performed experiments targeting the
43 human alpha satellite repeat DNA region in K29Mes cells (Fig. 2b) as well as a 200 kb single-
44 copy chromosomal region on Xp22.32 (hg38 chrX:5400000–5600000) using a previously
45 validated complex oligo library and an accompanying readout probe³¹ on primary human
46 metaphase chromosome spreads (Fig. 2c). In both cases, brightfield microscopy revealed
47 strong, punctate staining in the expected patterns specific to DNA, whereas no appreciable
48 staining was observed in the corresponding no primary probe controls (Fig. 2b,c). Finally, we
49 examined the ability of colorimetric pSABER to detect targets in FFPE tissue sections, which

1 represents the main specimen format in clinical and research pathology laboratories
2 worldwide. We first performed RNA ISH in deidentified human kidney FFPE sections using a
3 probe set consisting of 6 oligos targeting the internal transcribed spacer 1 (ITS1) region of the
4 47S pre-rRNA that is localized exclusively in the nucleolus³². After colorimetric development,
5 we observed tightly localized signal inside of nearly every nucleus in the section, with the
6 expected 1–2 signals per nucleus being observed (Fig. 2d). We also verified colorimetric RNA
7 pSABER can detect RNA originating from a non-repetitive locus in FFPE specimens by
8 performing RNA ISH with a probe set consisting of 83 oligos targeting the *UMOD* mRNA in
9 deidentified human kidney sections. Using pSABER we detected a very specific pattern of
10 *UMOD* transcript localization in cells of the thick ascending loop of Henle (TALH) (arrowheads,
11 Fig. 2e, center panel), but not in cells of the adjacent macula densa (MD), a specialized
12 structure in the vicinity of the kidney glomerulus-tubule junction. This localization pattern
13 exactly matched *UMOD* protein expression as determined by immunohistochemistry in the
14 human protein atlas³³. No detectable staining was observed in the corresponding no primary
15 probe controls for the kidney FFPE experiments (Fig. 2d,e). These experiments further
16 validated pSABER for *in situ* localization of mRNA molecules in clinically relevant samples.
17

18 Enhanced signal amplification with fluorescent pSABER

19 HRP can also catalyze covalent deposition of fluorophore-conjugated tyramides in a
20 variety of specimen types. Therefore, we next set out to determine whether pSABER could
21 generate amplified fluorescent signals *in situ* via the HRP-catalyzed deposition of fluorophore-
22 conjugated tyramides at the sites of primary probe binding. To this end, we performed a series
23 of fluorescent RNA pSABER experiments in EY.T4³⁴ mouse embryonic fibroblast cells using
24 fluorescein-tyramide (Methods). During the development step, we independently targeted each
25 of three RNA species with distinct expected spatial signal patterns: 1) the 47S rRNA ITS1
26 region that is localized exclusively in the nucleolus³² (Fig. 3a); 2) the 7SK small nuclear RNA
27 which is broadly localized within the nucleoplasm and enriched in nuclear speckles, but
28 excluded from nucleoli³⁵ (Fig. 3b); the *Cbx5* mRNA which localizes predominantly in the
29 cytoplasm²⁸ (Fig. 3c). In all three cases, using confocal microscopy, we observed the expected
30 staining patterns, whereas we saw no detectable signal in the no primary probe negative
31 control (Fig. 3b). We also validated that fluorescent pSABER can faithfully visualize nucleic acid
32 targets in FFPE specimens by performing an experiment targeting ITS1 in deidentified human
33 kidney FFPE tissue sections. This revealed the expected pattern of strong nucleolar staining
34 (Fig. 3e) that matched the signal seen with colorimetric DAB development (Fig. 2d) and that
35 was not observed in the matched no primary probe negative control (Fig. 3f).

36 After verifying that pSABER is readily compatible with fluorescent detection, we next
37 set out to quantify the degree of signal amplification provided by pSABER. In particular, we
38 aimed to measure how much, if any, additional amplification pSABER provides over the
39 conventional version of the SABER technique. To this end, we performed a paired series of ISH
40 experiments targeting the centromeric mouse minor satellite repeat in EY.T4 MEF cells in
41 which the same pool of PER-extended probe was hybridized and visualized either via the
42 recruitment of an ATTO 488 labeled oligo (SABER) or via the recruitment of an HRP-oligo
43 followed by development with fluorescein-tyramide (pSABER) (Fig. 4a). Both samples were
44 acquired using matched illumination and camera exposure settings. These settings were
45 optimized to utilize the full dynamic range of the camera without significant amounts of pixel
46 saturation (Methods), allowing a direct and quantitative comparison of the signal intensities of
47 each sample (Fig. 4b). Following automated segmentation nuclei and minor satellite FISH
48 puncta (Methods), pSABER was observed to produce a distribution of peak signal intensity per
49 puncta values whose median was 25.1x greater than the corresponding SABER distribution

1 (Fig. 4c). A similar fold-enhancement (21.3x) was observed when comparing the means of the
2 distributions (Fig. 4c). From these data, we conclude that fluorescent pSABER provides
3 substantial signal amplification (>20x) relative to conventional SABER. Furthermore, as SABER
4 was reported to produce ~10x signal amplification relative to unamplified FISH at similar
5 targets²⁸, we estimate that fluorescent pSABER provides >200x amplification relative to
6 unamplified FISH.

7

8 Exchange-pSABER for multiplexed detection with amplification

9 A powerful feature of SABER is its ability to sequentially visualize multiple targets via
10 the programmable displacement of bound fluorescently labeled oligos and the subsequent
11 hybridization of labeled oligos to distinct targets bearing orthogonal sequence extensions²⁸. We
12 reasoned that fluorescent pSABER could also harness this property to enable multiplexed and
13 highly amplified imaging via solution exchange of HRP-oligos between subsequent rounds of
14 signal development (Fig. 5a). To test this idea, we designed a 3-color imaging experiment
15 targeting the *Cbx5* mRNA, the 7SK small nuclear RNA, and the ITS1 region of the 47S rRNA. In
16 this experiment, all primary probes were first co-hybridized in a single overnight step. Next, we
17 added the HRP-oligo complementary to the “p27” SABER extension borne by the *Cbx5* probe
18 set and developed this with Cy5-tyramide (Fig. 5b, top). We then removed the bound HRP-
19 oligo by solution exchange into formamide buffer²⁸ (Methods), allowing us to perform a second
20 round of hybridization of with the HRP-oligo, but this time complementary to the “p30”
21 extension borne by the 7SK probe set and developed with Cy3-tyramide (Fig. 5b, middle). In
22 the final cycle, we removed the bound HRP-oligo via solution exchange and performed a third
23 round of hybridization and development at ITS1 with fluorescein-tyramide (Fig. 5c, bottom).
24 Visualization after each round of development revealed the sequential accumulation of
25 amplified signal patterns at the three targets, with the fluorescent tyramides added during
26 previous rounds remaining stable and prominently visible even during later rounds (Fig. 3b).
27 After the three rounds, we observed that signal associated with each RNA target was properly
28 localized to the correct subcellular location with minimal spatial overlap even when visualized
29 using “SoRa” super-resolution spinning disc confocal microscopy (Fig. 3c). Moreover, we
30 found that we could observe the amplified, multiplexed staining pattern even when using lower
31 numerical aperture air objectives on an automated slide scanning microscope at 40x, 20x and
32 even 10x magnifications (Fig. 4d), whereas we were essentially unable to detect conventional
33 SABER using the same system (Supplementary Fig. 1).

34

35

36 Discussion

37 The pSABER approach sits conveniently upon the established PER/SABER platform to
38 expand its capabilities to colorimetric detection and highly amplified (>200x) multiplexing at up
39 to three molecular targets. The use of an HRP-oligo integrates seamlessly into the SABER FISH
40 workflow and only adds a brief (~10 min) hydrogen peroxide incubation prior to sample
41 permeabilization to inactive endogenous peroxidases and a short series of washes (~10-30
42 mins) after development by HRP to remove residual HRP substrate. The use of the HRP-oligo
43 and tyramide substrates is effectively cost-equivalent to performing conventional SABER,
44 increasing the cost of visualization reagents per sample from ~\$0.10–\$0.60 per sample
45 (SABER) to \$0.45–\$2.30 per sample depending on the scale of the experiment (Table 1); in
46 both cases, the cost of these development reagents is a minor fraction of the overall cost of
47 the SABER/pSABER ISH experiment. We have demonstrated that pSABER: a) is readily
48 compatible with colorimetric detection and histopathological stains, b) can substantially
49 amplify target signals >20x beyond conventional SABER while maintaining expected

1 subcellular localization patterns, c) can be multiplexed via solution exchange, d) is compatible
2 with a broad range of optical systems including those commonly found in clinical labs, e) and
3 can reveal detailed information about the spatial distribution of nucleic acid targets even on low
4 numerical aperture and low magnification platforms. Given the simplicity, robustness and
5 flexible readout options of the pSABER approach, we anticipate that it will serve as an enabling
6 imaging technology in a wide set of clinical and research settings.

7

8

9 Methods

10

11 Cell culture

12 K29Mes human kidney mesangial cells³⁰ were obtained from M. Saleem (University of Bristol)
13 and cultured in RPMI-1640 medium supplemented with 10% (vol/vol) FBS, 1x L-glutamine, 1x
14 non-essential amino acids, ITS+ supplement, and 50 U/ml penicillin, and 50 µg /ml
15 streptomycin. K29Mes cells were grown at 33°C (permissive temperature) and were then
16 shifted to 37°C (nonpermissive temperature) before fixation causing degradation of the
17 temperature sensitive SV40 T-antigen to promote growth arrest and differentiation. Prior to
18 experiments, cells were either seeded on 22 x 22 mm #1.5 coverslips in 6-well plates at a
19 density of about 100,000 cells per well or seeded on Ibidi 8-well chamber slides at a density of
20 about 70,000 and kept at 37°C overnight to allow adherence to coverslips. Cells were then
21 rinsed in 1x PBS, fixed in either 4% (wt/vol) paraformaldehyde in 1x PBS or 10% (vol/vol)
22 neutral buffered formalin for 10 minutes at room temperature, then rinsed twice in 1x PBS.
23 EY.T4³⁴ mouse embryonic fibroblast cells mouse embryonic fibroblast cells were grown in
24 DMEM (ThermoFisher 10566016) supplemented with 15% (vol/vol) FBS (ThermoFisher
25 A3160502), 50 U/ml penicillin, and 50 µg /ml streptomycin (ThermoFisher 15140122) 37°C in
26 the presence of 5% CO₂.

27

28 Tissue

29 All deidentified human kidney tissue samples used in experiments were from the renal cortex
30 region of the kidney obtained through nephrectomies performed at the University of
31 Washington hospitals with local institutional review board approval (STUDY00001297). Fresh
32 tissue was fixed for a minimum of 8 hours-overnight in 10% (vol/vol) neutral buffered formalin
33 followed by rinsing in H₂O and storage in 70% EtOH at 4°C till paraffin embedding. After
34 embedding, 5 µm sections were obtained and placed on positively-charged microscope slides.

35

36 FISH probes

37 Oligo probes targeting the human alpha satellite repeat, the human and mouse ITS1 RNA, the
38 mouse 7SK RNA, and the mouse minor satellite repeat were purchased as individually column-
39 synthesized DNA oligos from Integrated DNA Technologies. Probe sets targeting the human
40 ADAMTS1 mRNA, the human UMOD mRNA, and the mouse Cbx5 mRNA were designed using
41 PaintSHOP³¹ and ordered in plate oligo or oPool format from Integrated DNA Technologies.
42 The complex oligo library used to target Xp22.32 was purchased from Twist Biosciences and
43 amplified and processed as described previously³¹. The sequences of the oligos probes used
44 are listed in Supplementary Dataset 1.

45

46 Primer exchange reaction

47 To extend FISH probes into PER concatemers, 100 µl reactions were set up containing 1x
48 PBS, 10mM MgSO₄, 300 µM dNTP mix (dA, dC and dT only), 100 nM Clean.G hairpin, 40-600
49 U/mL of Bst LF polymerase (New England Biolabs), 500 nM of hairpin, and water to 90 µl.

1 Reactions were incubated for 15 minutes at 37°C, then 10 µl of 10 µM of primer was added to
2 each reaction and incubated at 37°C for 2 hours, followed 20 minutes at 80°C to heat-
3 inactivate the polymerase. To check the success of extensions and concatemer lengths,
4 samples (diluted in 2x Novex TBE-Urea sample buffer) and DNA ladders (Low Range and 100
5 bp or 1 kb Plus, Thermo Fisher Scientific) were boiled at 95°C for 5 minutes then were run on
6 10-15% TBE-Urea gels for 30-60 minutes at 70°C using a circulating water bath hooked up to
7 the gel cassette. Reactions were dehydrated via vacuum evaporation for long-term storage (at
8 room temperature) and resuspended in hybridization solutions for downstream F/ISH
9 experiments.

10

11 **Colorimetric DNA pSABER in fixed tissue culture cells**

12 Fixed samples were permeabilized in 1x PBS with 0.1% (vol/vol) Triton X-100 for 10 minutes at
13 room temperature, rinsed in 1x PBS, incubated in 0.5% (vol/vol) H₂O₂ in 1x PBS for 10 minutes,
14 rinsed twice with 1x PBS, treated with 0.1N HCl for 5 minutes and washed twice with 2x SSC
15 plus 0.1% (vol/vol) Tween-20 (2x SSCT). Coverslips were incubated in 2x SSCT with 50%
16 (vol/vol) formamide for 2 minutes at room temperature and again for 20 minutes at 60°C.
17 Samples were then inverted onto 25 µl of primary hybridization solution made up of 2x SSCT,
18 0.1% (vol/vol) Tween-20, 50% (vol/vol) formamide, 10% (wt/vol) dextran sulfate, 400 ng/µl of
19 RNaseA, and 92 µl of dried PER reaction. Coverslips were placed in a humidified chamber,
20 denatured at 78°C on a water-immersed heat block 3 minutes and then transferred to a
21 benchtop air incubator for overnight incubation at 45°C. After hybridization with primary
22 probes, samples were rinsed quickly in pre-warmed 2x SSCT before 4 rounds of 5-minute
23 washes at 60°C and then 2 rounds of 2-minute washes in 2x SSCT at room temperature. For
24 secondary hybridization (colorimetric detection), samples were rinsed in 1x PBS, incubated in
25 blocking solution (1% wt/vol BSA and 0.1% vol/vol Tween-20 in 1x PBS), washed with 1x PBS
26 twice, and inverted onto 25 µl of secondary hybridization solution consisting of 2x SSCT, 0.1%
27 (vol/vol) Tween-20, 30% (vol/vol) formamide, 10% (wt/vol) dextran sulfate, and 100 nM HRP-
28 oligo held at 37°C for 1 hour. Following secondary hybridization, coverslips were washed twice
29 for 5 minutes in 1x PBS with 0.1% (vol/vol) Tween-20 at 37°C followed by a 5-minute wash in
30 1x PBS at room temperature. To develop color, samples were inverted onto 25 µl of DAB
31 solution (1 drop of DAB Chromogen plus 50 drops of DAB substrate—Abcam ab64238) for 30
32 minutes, washed twice with tap water, counterstained with hematoxylin for 1 minute, rinsed
33 with tap water twice, washed with 0.002% (vol/vol) ammonia water, and then washed in 70%,
34 95% and 100% (vol/vol) ethanol for a 3–5 mins each. To mount coverslips, they were each
35 dipped in xylene 5 times and inverted onto a microscope slide holding a few drops of
36 CytoSeal-XYL mounting medium. Mounted coverslips were kept in a microscope slide case at
37 room temperature prior to imaging.

38

39 **Colorimetric DNA pSABER on metaphase spreads**

40 Carrying out colorimetric DNA pSABER on human metaphase chromosome spreads was
41 similar to the ‘Colorimetric DNA pSABER in fixed tissue culture cells’ protocol except for the
42 steps taken right before primary probe hybridization. Slides with metaphase spreads were
43 taken out of the -20°C freezer and denatured in 2x SSCT + 70% (vol/vol) formamide at 70°C
44 for 3 minutes, followed by a 5-minute wash in ice-cold 70% (vol/vol) ethanol, in 90% (vol/vol)
45 ethanol and in 100% ethanol and then allowed to air-dry before applying hybridization solution.

46

47 **Colorimetric RNA pSABER in fixed tissue culture cells**

48 Fixed samples were permeabilized in 1x PBS with 0.1% (vol/vol) Triton X-100 for 10 minutes at
49 room temperature, rinsed in 1x PBS, incubated in 0.5% (vol/vol) H₂O₂ in 1x PBS for 10 minutes,

1 rinsed twice with 1x PBS, washed once with 1x PBS containing 0.1% (vol/vol) Tween (PBST),
2 and once with 2x SSCT. Samples were then inverted onto 25 μ l of primary hybridization
3 solution made up of 2x SSCT, 0.1% (vol/vol) Tween-20, 10-40% (vol/vol) formamide, 10%
4 dextran sulfate, and 92 μ l of dried PER reaction. Coverslips were placed in a humidified
5 chamber, denatured at 60°C on a water-immersed heat block for 3 minutes and then
6 transferred to a benchtop air incubator for overnight incubation at 42°C. After hybridization
7 with primary probes, samples were rinsed quickly in pre-warmed 2x SSCT before 4 rounds of
8 5-minute washes at 60°C and then 2 rounds of 2-minute 2x SSCT washes at room
9 temperature. For secondary hybridization (colorimetric detection), samples were rinsed in 1x
10 PBS, incubated in blocking solution (1% wt/vol BSA and 0.1% vol/vol Tween-20 in 1x PBS),
11 washed with 1x PBS twice and inverted onto 25 μ l of secondary hybridization solution
12 consisting of 2x SSCT, 0.1% (vol/vol) Tween-20, 30% (vol/vol) formamide, 10% (wt/vol)
13 dextran sulfate and 100nM HRP-oligo and held at 37°C for 1 hour in the dark. Following
14 secondary hybridization, coverslips were washed twice for 5 minutes in PBST at 37°C followed
15 by a 5-minute wash in 1x PBS at room temperature. To develop color, samples were inverted
16 onto 25 μ l of DAB solution (1 drop of DAB Chromogen plus 50 drops of DAB substrate for 30
17 minutes, washed twice with tap water, counterstained with hematoxylin for 1 minute, rinsed
18 with tap water twice, washed with 0.002% (vol/vol) ammonia water, and then washed in 70%,
19 95% and 100% (vol/vol) ethanol for a few minutes each. To mount coverslips, they were each
20 dipped in xylene 5 times and inverted onto a microscope slide holding a few drops of
21 CytoSeal-XYL mounting medium for. Mounted coverslips were kept in a microscope slide case
22 at room temperature prior to imaging.
23

24 **Colorimetric RNA pSABER in FFPE tissue**

25 To deparaffinize FFPE sections, slides were placed in a slide rack and submerged in xylene
26 twice for five minutes, incubated in 100% ethanol twice for 1 minute then removed and allowed
27 to be air dried for 5 minutes at room temperature. To prepare FFPE tissue sections for *in situ*
28 hybridization, pretreatment reagents from Advanced Cell Diagnostics (ACD) were used.
29 Sections were incubated in 5–8 drops of ACD's hydrogen peroxide for 10 minutes at room
30 temperature and rinsed with distilled water twice. The tissue slides were then submerged into
31 the boiling 1x Target Retrieval solution from ACD for 10 minutes and immediately transferred to
32 a staining dish containing distilled water, followed by another water rinse. Slides were washed
33 in 100% ethanol quickly and allowed to be air dried. Lastly, sections were incubated with
34 ACD's Protease Plus, placed in a humidified chamber inside an air incubator at 40°C for 40
35 minutes and washed with distilled water twice. Pretreatment steps were followed by primary
36 probe hybridization and all the following steps detailed in the protocol for 'Colorimetric RNA
37 pSABER in fixed tissue culture cells' protocol.
38

39 **Fluorescent RNA pSABER in fixed tissue culture cells**

40 Fixed cells that were grown on Ibidi 8-well chamber slides underwent the same steps
41 described in the 'Colorimetric RNA pSABER in fixed tissue culture cells' protocol up to the
42 wash prior to undergoing secondary hybridization. For the secondary hybridization 125 μ l of
43 secondary hybridization solution consisting of 2x SSCT, 0.1% (vol/vol) Tween-20, 10% (wt/vol)
44 dextran sulfate and 100nM HRP-oligo was added to the samples and held at 37°C for 1 hour in
45 the dark. Cells in each well were then washed 3 times for 5 minutes in PBST at 37°C. To
46 employ signal amplification via tyramide, fluorescent tyramide reagents that were purchased
47 from Tocris were optimized and final concentrations of 480nM, 1.1 μ M, and 3.75 μ M for
48 fluorescein, cy3 and cy5 tyramides were established respectively. To develop signal, 125 μ l of
49 tyramide solution consisting of 1x PBS, 0.0015% (vol/vol) H_2O_2 , and one of the fluorescent

1 tyramides was added to the samples for 10 minutes at room temperature. To quench enzyme
2 activity, samples were washed 3 times for 5 minutes with a quenching solution containing 10
3 mM sodium azide and 10 mM sodium ascorbate in PBST and 2 extra washes with PBST alone.
4 Prior to being imaged, 125 μ l of SlowFade Gold Antifade Mountant with DAPI was added to
5 each well.
6

7 **DNA SABER-FISH and Fluorescent DNA pSABER in fixed tissue culture cells**

8 DNA FISH was performed essentially as described previously²⁸. Cells were grown on Ibidi 18-
9 well chamber slides at a seeding density of ~7000 cells/ well in a mammalian tissue culture
10 incubator and fixed in 4% (wt/vol) paraformaldehyde for 10 minutes. The samples were
11 permeabilized in 1x PBS + 0.5% (vol/vol) Triton x-100 for 10 minutes at room temperature
12 (hereafter RT), rinsed in 1x PBS + 0.1% Tween-20 (hereafter PBS-T) for 5 minutes, incubated in
13 0.1N HCl for 5 minutes, rinsed with PBS-T, incubated in 3% (vol/vol) H₂O₂ in PBS-T for 10
14 minutes (pSABER only), rinsed twice with 2x SSC + 0.1% (vol/vol) Tween-20 (hereafter 2x
15 SSCT), incubated in 2x SSCT + 50% (vol/vol) formamide for 2 minutes, incubated in 2x SSCT+
16 50% (vol/vol) formamide at 60°C for 20 minutes on a water-immersed heat block, and
17 denatured at 80°C for 3 minutes in a hybridization solution consisting of 2x SSC, 0.1% (vol/vol)
18 Tween-20, 50% (vol/vol) formamide, 10% (wt/vol) dextran sulfate, 0.4ug/uL RNase A, and 100
19 pmol of unpurified PER reaction. The slide was then held at 37°C overnight in a humidified
20 chamber. On the next day, 4 washes' worth of 2x SSCT were pre-warmed to 60°C and the
21 cells were rinsed twice with RT 2x SSCT. The cells were then rinsed 4x with the pre-warmed
22 2xSSCT on a 60° heat block, with each rinse taking 5 minutes. This was followed by two quick
23 RT rinses with 2x SSCT and three quick rinses in 1x PBS. The cells were then incubated at
24 37°C for 1 hour in a secondary hybridization solution consisting of 0.1uM fluor oligos (SABER)
25 or HRP-oligos (pSABER) in 1x PBS. During this hour, three washes' worth of PBS-T were pre-
26 warmed to 37°C. After the secondary hybridization was complete, the cells were rinsed 3x in
27 the pre-warmed PBS-T, with each wash taking 5 minutes. For pSABER, cells were then
28 incubated for 10 minutes at RT in a labeling solution consisting of fluorescein tyramide (Torcis
29 6456) diluted 1:50,000 from its 24 mM stock and 0.0015% (vol/vol) H₂O₂ in PBS-T. pSABER
30 development, the cells were rinsed 3x for 5 minutes each in a reaction quenching solution
31 consisting of 10mM sodium ascorbate and 10mM sodium azide in PBS-T. Finally, the cells
32 were rinsed twice in PBS-T and SlowFade Gold antifade mountant with DAPI was added.
33

34 **Fluorescent RNA pSABER in FFPE tissue**

35 FFPE tissue sections underwent the same deparaffinization and pretreatment steps detailed in
36 the protocol for Colorimetric RNA pSABER in FFPE tissue. Following pretreatment incubations,
37 tissue samples went through the same stages laid out in the protocol for 'Fluorescent RNA
38 pSABER in fixed tissue culture cells', however, they did not get SlowFade Gold Antifade
39 Mountant with DAPI at the end. Prior to imaging, tissue slices were stained with 0.1 ug/mL
40 DAPI (in 1x PBS) for 5 minutes and washed with 1x PBS. To reduce autofluorescence, the
41 samples were then treated with 1x TruBlack Lipofuscin Autofluorescence Quencher (in 70%
42 ethanol) for 1 minute taking care not to dry the tissue sections. Slides were washed 3 times
43 with 1x PBS and coverslips were mounted using Prolong Gold Antifade Mountant.
44

45 **Exchange RNA pSABER in fixed tissue culture cells**

46 The steps are identical to the steps of the 'Fluorescent RNA pSABER in fixed tissue culture
47 cells' protocol, but instead of adding the mountant with DAPI at the end, the samples were
48 washed with 60% (vol/vol) formamide in PBST for 15 minutes at room temperature to remove
49 the first round of HRP-oligo, followed by 2 washes with 1x PBS for 1 minute, another 2 washes

1 for 2 minutes and a final 5-minute wash. To enable another round of detection, samples were
2 incubated with BSA blocking solution again, and got 125 μ l of the second HRP-oligo
3 hybridization solution followed by all the steps detailed in the ‘Fluorescent RNA pSABER in
4 fixed tissue culture cells’ protocol that came after secondary hybridization. At the end either
5 another round of detection was performed or 125 μ l of SlowFade Gold Antifade Mountant with
6 DAPI was added to each well prior to imaging. The following three tyramides were used:
7 fluorescein at 1:50,000 from the 24 mM stock (Tocris 6456); Cy3 at 1:15,0000 from the 16 mM
8 stock (Tocris 6457); Cy5 (Tocris 6458) at 1:4,000 from the 15 mM stock.
9

10 **Microscopy**

11 Transmitted light microscopy of colorimetric pSABER samples was performed on an Olympus
12 BX41 upright microscope using 20x Plan N.A. 0.25, 40x UPlan N.A. 0.75 or 60x Ach N.A. 0.80
13 air objectives with images captured using a Leica DFC420 camera. Confocal imaging of
14 fluorescent SABER and pSABER samples was performed using Yokogawa CSU-W1 SoRa
15 spinning disc confocal attached to a Nikon Eclipse Ti-2 microscopy. Excitation light was
16 emitted at 30% of maximal intensity from 405 nm, 488 nm, 561 nm, or 640 nm lasers housed
17 inside of a Nikon LUNF 405/488/561/640NM 1F commercial launch. Laser excitation was
18 delivered via a single-mode optical fiber into the into the CSU-W1 SoRa unit. Excitation light
19 was then directed through a microlens array disc and a ‘SoRa’ disc containing 50 μ m pinholes
20 and directed to the rear aperture of a 100x N.A. 1.49 Apo TIRF oil immersion objective lens by
21 a prism in the base of the Ti2. Emission light was collected by the same objective and passed
22 via a prism in the base of the Ti2 back into the SoRa unit, where it was relayed by a 1x lens
23 (conventional imaging) or 2.8x lens (super-resolution imaging) through the pinhole disc and
24 then directed into the emission path by a quad-band dichroic mirror (Semrock Di01-
25 T405/488/568/647-13x15x0.5). Emission light was then spectrally filtered by one of four single-
26 bandpass filters (DAPI: Chroma ET455/50M; ATTO 488: Chroma ET525/36M; ATTO 565:
27 Chroma ET605/50M; Alexa Fluor 647: Chroma ET705/72M) and focused by a 1x relay lens onto
28 an Andor Sona 4.2B-11 camera with a physical pixel size of 11 μ m, resulting in an effective
29 pixel size of 110 nm (conventional) or 39.3 nm (super-resolution). The Sona was operated in
30 16-bit mode with rolling shutter readout and exposure times of 70–300 ms. Automated slide-
31 scanning microscopy was performed on a Keyence BZ-X800. Excitation light from the
32 integrated white light source was emitted at 25% of maximal intensity, passed through the ‘ET
33 DAPI’, ‘ET GFP’, ‘Cy3’, or ‘Cy5’ filter cube for excitation band filtering and was directed to the
34 sample by a 10x N.A. 0.45 Plan Apo, 20x N.A. Plan Apo, or 40x N.A. 0.95 air objective lens.
35 Emission light was collected by one of the objective lenses and directed into the microscope’s
36 emission path by one of the filter cubes, after which it was spectrally filtered while exiting the
37 filter cube and focused by a 1x relay lens onto an integrated CCD camera with a physical pixel
38 size of 7.549 μ m, resulting in effective pixels sizes of 188.7 nm (40x), 377.4 nm (20x), or 754.9
39 nm (10x). The CCD camera was operated in 14-bit mode without pixel binning and exposure
40 times of 16.7–666.7 ms. Images were processed in ImageJ/Fiji^{36,37} and Adobe Photoshop.
41

42 **Quantitative analysis of peak puncta intensities**

43 We developed an image analysis pipeline to detect and segment puncta from both SABER and
44 pSABER experiments quantify their peak intensities. The pipeline is capable of loading .nd2
45 image files containing channels with a nuclear stain (here DAPI) and fluorescent puncta,
46 segmenting nuclei in 2D and detecting puncta inside the nuclei, and returning raw intensity
47 values for each punctum. Each image is first loaded with the nd2reader python package, and
48 DAPI / GFP channels are split for separate processing pathways. For the DAPI channel, 2D

1 segmentation was performed with the python package StarDist, specifically the
2 “2D_versatile_fluo” pretrained model^{38,39}. To generate more accurate segmentation results,
3 nuclear segmentation was performed on a max-intensity projection which was downsampled
4 by a factor of 16. The resulting segmentation mask was then upsampled to the original
5 resolution. For the GFP channel, a maximum-intensity projection was generated and spot
6 detection was performed using the *blob_log* function from scikit-image⁴⁰. Spot detection with
7 *blob_log* consisted of fitting a 2D Gaussian distribution to each punctum and returned the
8 highest-intensity pixel as the 16-bit intensity of the spot. For SABER, sigma parameters were
9 set as follows: threshold = 0.02, min_sigma=0.001, max_sigma=0.5, num_sigma=20. For
10 pSABER, sigma parameters were set as: min_sigma=0.01, max_sigma=1, num_sigma=20.
11 Detected spots were then filtered based on overlap with the nuclear segmentation mask. Data
12 from each condition was aggregated and visualized with matplotlib. To quantify signal
13 amplification, the cumulative distribution function for the SABER and pSABER spot intensities
14 was generated, and the distributions were normalized to the SABER condition (median = 1).
15 Signal amplification here was defined as the resulting median of the pSABER distribution.
16
17

18 **Code and Data Availability**

19 The source code for the automated analysis of peak puncta intensities as well as example
20 input images is available at <https://github.com/beliveau-lab/SABER-Spot-Quant> under a MIT
21 license. Additional primary microscopy data will be made available upon request.
22

23 **Author Contributions**

24 S. Attar, S. Akilesh, and B.J.B. conceived the study. V.A.B. wrote and optimized software code.
25 S. Attar, V.A.B., E.K.N., and A.F.T. performed experiments. S. Attar, V.A.B., S. Akilesh, and
26 B.J.B. wrote the manuscript. All authors edited and approved the manuscript. D.M.S., J.S.,
27 J.A.L., S. Akilesh, and B.J.B. supervised the work.
28
29

30 **Competing Interests**

31 S. Attar, A.F.T., D.M.S., S. Akilesh, and B.J.B. have filed a patent application covering
32 pSABER. B.J.B. is listed as an inventor on patent applications related to the SABER
33 technology.
34
35

36 **Acknowledgements**

37 The authors thank members of the Shechner, Shendure, Lieberman, Akilesh, and Beliveau labs
38 for helpful discussion about this work. We thank N. Peters of the UW W.M. Keck Microscopy
39 Center and D. Fong of Nikon for assistance with microscopy during the development of
40 pSABER and S. Jiang for helpful advice about working with HRP in tissues. This work was
41 supported by a Damon Runyon Dale F. Frey Breakthrough Award (32-19 to B.J.B.), the
42 National Institutes of Health (under grants 1R35GM137916 to B.J.B, 1UM1HG011586 to J.S.
43 and B.J.B., 1R01DK130386 to S. Akilesh, 1R01GM138799-01 to D.M.S.), the Andy Hill Cancer
44 Research Endowment (under a COVID-19 Response Grant Award to B.J.B. and S. Akilesh),
45 and the Diabetic Complications Consortium (under grant 19AU3987 to S. Akilesh and B.J.B.).
46 This project was also supported in part by a Building Bridges Award to J.A.L. and S. Akilesh

1 from the Department of Laboratory Medicine and Pathology. A.F.T. was supported by NIH
2 training grant T32GM007750.

3
4

5 **References**

- 7 1. Pardue, M. L. & Gall, J. G. Molecular hybridization of radioactive DNA to the DNA of
8 cytological preparations. *Proc. Natl. Acad. Sci. U. S. A.* **64**, 600–604 (1969).
- 9 2. Riegel, M. Human molecular cytogenetics: From cells to nucleotides. *Genetics and*
10 *Molecular Biology* vol. 37 194–209 Preprint at <https://doi.org/10.1590/S1415-47572014000200006> (2014).
- 12 3. Raj, A., van den Bogaard, P., Rifkin, S. a., van Oudenaarden, A. & Tyagi, S. Imaging
13 individual mRNA molecules using multiple singly labeled probes. *Nat. Methods* **5**, 877–879
14 (2008).
- 15 4. Solovei, I. *et al.* Spatial preservation of nuclear chromatin architecture during three-
16 dimensional fluorescence *in situ* hybridization (3D-FISH). *Exp. Cell Res.* **276**, 10–23 (2002).
- 17 5. Rosen, B. & Beddington, R. S. Whole-mount *in situ* hybridization in the mouse embryo:
18 gene expression in three dimensions. *Trends Genet.* **9**, 162–167 (1993).
- 19 6. Rudkin, G. T. & Stollar, B. D. High resolution detection of DNA-RNA hybrids *in situ* by
20 indirect immunofluorescence [29]. *Nature* vol. 265 472–473 Preprint at
21 <https://doi.org/10.1038/265472a0> (1977).
- 22 7. Bauman, J. G. J., Wiegant, J., Borst, P. & van Duijn, P. A new method for fluorescence
23 microscopical localization of specific DNA sequences by *in situ* hybridization of
24 fluorochrome-labelled RNA. *Exp. Cell Res.* **128**, 485–490 (1980).
- 25 8. Langer-Safer, P. R., Levine, M. & Ward, D. C. Immunological method for mapping genes
26 on *Drosophila* polytene chromosomes. *Proc. Natl. Acad. Sci. U. S. A.* **79**, 4381–4385
27 (1982).
- 28 9. Rigby, P. W. J., Dieckmann, M., Rhodes, C. & Berg, P. Labeling deoxyribonucleic acid to
29 high specific activity *in vitro* by nick translation with DNA polymerase I. *J. Mol. Biol.* **113**,
30 237–251 (1977).
- 31 10. Femino, a. M., Fay, F. S., Fogarty, K. & Singer, R. H. Visualization of single RNA transcripts
32 *in situ*. *Science* **280**, 585–590 (1998).
- 33 11. Yamada, N. A. *et al.* Visualization of fine-scale genomic structure by oligonucleotide-based
34 high-resolution FISH. *Cytogenet. Genome Res.* **132**, 248–254 (2011).
- 35 12. Boyle, S., Rodesch, M. J., Halvensleben, H. A., Jeddeloh, J. A. & Bickmore, W. A.
36 Fluorescence *in situ* hybridization with high-complexity repeat-free oligonucleotide probes
37 generated by massively parallel synthesis. *Chromosome Res.* **19**, 901–909 (2011).
- 38 13. Beliveau, B. J. *et al.* Versatile design and synthesis platform for visualizing genomes with
39 Oligopaint FISH probes. *Proceedings of the National Academy of Sciences* **109**, 21301–
40 21306 (2012).
- 41 14. Lubeck, E., Coskun, A. F., Zhiyentayev, T., Ahmad, M. & Cai, L. Single-cell *in situ* RNA
42 profiling by sequential hybridization. *Nature methods* vol. 11 360–361 (2014).

- 1 15. Chen, K. H., Boettiger, A. N., Moffitt, J. R., Wang, S. & Zhuang, X. RNA imaging. Spatially
2 resolved, highly multiplexed RNA profiling in single cells. *Science* **348**, aaa6090 (2015).
- 3 16. Wang, S. *et al.* Spatial organization of chromatin domains and compartments in single
4 chromosomes. *Science* **353**, 598–602 (2016).
- 5 17. Jensen, E. Technical Review: In Situ Hybridization. *Anat. Rec.* **297**, 1349–1353 (2014).
- 6 18. McNicol, A. M. & Farquharson, M. A. In situ hybridization and its diagnostic applications in
7 pathology. *J. Pathol.* **182**, 250–261 (1997).
- 8 19. Player, A. N., Shen, L. P., Kenny, D., Antao, V. P. & Kolberg, J. A. Single-copy gene
9 detection using branched DNA (bDNA) in situ hybridization. *J. Histochem. Cytochem.* **49**,
10 603–611 (2001).
- 11 20. Wang, F. *et al.* RNAscope: A novel in situ RNA analysis platform for formalin-fixed,
12 paraffin-embedded tissues. *J. Mol. Diagn.* **14**, 22–29 (2012).
- 13 21. Beliveau, B. J. *et al.* Single-molecule super-resolution imaging of chromosomes and in situ
14 haplotype visualization using Oligopaint FISH probes. *Nat. Commun.* **6**, 7147 (2015).
- 15 22. Choi, H. M. T. *et al.* Programmable in situ amplification for multiplexed imaging of mRNA
16 expression. *Nat. Biotechnol.* **28**, 1208–1212 (2010).
- 17 23. Rouhanifard, S. H. *et al.* ClampFISH detects individual nucleic acid molecules using click
18 chemistry-based amplification. *Nat. Biotechnol.* (2018) doi:10.1038/nbt.4286.
- 19 24. Dardani, I. *et al.* ClampFISH 2.0 enables rapid, scalable amplified RNA detection in situ.
20 *Nat. Methods* **19**, 1403–1410 (2022).
- 21 25. Kerstens, H. M., Poddighe, P. J. & Hanselaar, a. G. A novel in situ hybridization signal
22 amplification method based on the deposition of biotinylated tyramine. *J. Histochem.
23 Cytochem.* **43**, 347–352 (1995).
- 24 26. Schulte-Merker, S., Ho, R. K., Herrmann, B. G. & Nüsslein-Volhard, C. The protein product
25 of the zebrafish homologue of the mouse T gene is expressed in nuclei of the germ ring
26 and the notochord of the early embryo. *Development* **116**, 1021–1032 (1992).
- 27 27. Lizardi, P. M. *et al.* Mutation detection and single-molecule counting using isothermal
28 rolling-circle amplification. *Nature Genetics* vol. 19 225–232 Preprint at
29 <https://doi.org/10.1038/898> (1998).
- 30 28. Kishi, J. Y. *et al.* SABER amplifies FISH: enhanced multiplexed imaging of RNA and DNA in
31 cells and tissues. *Nat. Methods* (2019) doi:10.1038/s41592-019-0404-0.
- 32 29. Kishi, J. Y., Schaus, T. E., Gopalkrishnan, N., Xuan, F. & Yin, P. Programmable
33 autonomous synthesis of single-stranded DNA. *Nat. Chem.* (2017)
34 doi:10.1038/nchem.2872.
- 35 30. Sarrab, R. M. *et al.* Establishment of conditionally immortalized human glomerular
36 mesangial cells in culture, with unique migratory properties. *Am. J. Physiol. Renal Physiol.*
37 **301**, F1131–8 (2011).
- 38 31. Hershberg, E. A. *et al.* PaintSHOP enables the interactive design of transcriptome- and
39 genome-scale oligonucleotide FISH experiments. *Nat. Methods* **18**, 937–944 (2021).
- 40 32. Rouquette, J., Choesmel, V. & Gleizes, P.-E. Nuclear export and cytoplasmic processing
41 of precursors to the 40S ribosomal subunits in mammalian cells. *EMBO J.* **24**, 2862–2872

1 (2005).

2 33. Uhlén, M. *et al.* Proteomics. Tissue-based map of the human proteome. *Science* **347**,
3 1260419 (2015).

4 34. Yildirim, E., Sadreyev, R. I., Pinter, S. F. & Lee, J. T. X-chromosome hyperactivation in
5 mammals via nonlinear relationships between chromatin states and transcription. *Nat.*
6 *Struct. Mol. Biol.* **19**, 56–61 (2011).

7 35. Prasanth, K. V. *et al.* Nuclear organization and dynamics of 7SK RNA in regulating gene
8 expression. *Mol. Biol. Cell* **21**, 4184–4196 (2010).

9 36. Schneider, C. A., Rasband, W. S. & Eliceiri, K. W. NIH Image to ImageJ: 25 years of image
10 analysis. *Nat. Methods* **9**, 671–675 (2012).

11 37. Schindelin, J. *et al.* Fiji: an open-source platform for biological-image analysis. *Nat.*
12 *Methods* **9**, 676–682 (2012).

13 38. Schmidt, U., Weigert, M., Broaddus, C. & Myers, G. Cell Detection with Star-Convex
14 Polygons. in *Medical Image Computing and Computer Assisted Intervention – MICCAI*
15 2018 265–273 (Springer International Publishing, 2018).

16 39. Weigert, Schmidt, Haase, Sugawara & Myers. Star-convex Polyhedra for 3D Object
17 Detection and Segmentation in Microscopy. in *2020 IEEE Winter Conference on*
18 *Applications of Computer Vision (WACV)* vol. 0 3655–3662 (2020).

19 40. van der Walt, S. *et al.* scikit-image: image processing in Python. *PeerJ* **2**, e453 (2014).

20
21 **Figure Legends**

22
23 **Fig. 1 | Schematic overview of pSABER.** *In vitro* extended primary oligo probes are applied to
24 samples and hybridized *in situ* to DNA or RNA targets, facilitating the recruitment of a
25 secondary oligo conjugated with horseradish peroxidase (HRP) that can locally catalyze the
26 deposition of colorimetric or fluorescent labels.

27
28 **Fig. 2 | pSABER enables colorimetric detection of nucleic acid targets.** **a**, Visualization of
29 the ADAMTS1 mRNA in human K29Mes cells. **b**, Visualization of alpha satellite DNA in mRNA
30 in human K29Mes cells. **c**, Visualization of a 200 kb genomic interval within Xp22.32 on primary
31 human metaphase chromosome spreads. **d**, Visualization of ribosomal RNA internal
32 transcribed spacer 1 (ITS1) region in deidentified primary human paraffin fixed, formalin
33 embedded (FFPE) kidney tissue sections. **e**, Visualization of the UMOD mRNA in deidentified
34 primary human FFPE kidney tissue sections. A no primary probe negative control image
35 processed in parallel to each sample is shown to the left of each pSABER image. Scale bars,
36 20 µm (insets) or 50 µm (fields of view). MD = macula densa. TALH = thick ascending loop of
37 Henle.

38
39 **Fig. 3 | Fluorescent pSABER visualizes nucleic acid targets in cells and tissues.** **a**, DNA
40 (DAPI, left), fluorescent pSABER targeting the ribosomal RNA internal transcribed spacer 1
41 (ITS1) region performed in EY.T4 mouse embryonic fibroblasts (MEFs) (center), and a
42 composite image (right). **b**, DNA (DAPI, left), fluorescent pSABER targeting the 7SK RNA
43 performed in EY.T4 MEFs (center), and a composite image (right). **c**, DNA (DAPI, left),
44 fluorescent pSABER targeting the Cbx5 mRNA performed in EY.T4 MEFs (center), and a

1 composite image (right). **d**, DNA (DAPI, left), a no primary probe control for pSABER performed
2 in EY.T4 MEFs (center), and a composite image (right). **e**, DNA (DAPI, left), fluorescent pSABER
3 targeting ITS1 performed in deidentified primary human paraffin fixed, formalin embedded
4 (FFPE) kidney tissue sections (center), and a composite image (right). **f**, DNA (DAPI, left), a no
5 primary probe control for pSABER performed in deidentified primary human FFPE kidney
6 tissue sections (center), and a composite image (right). Each set of images is presented at the
7 indicated high (top) and low (bottom) contrast settings to allow for visual comparisons between
8 signals occupying different portions of the 16-bit dynamic range (0–65535). Images are
9 maximum projections in Z. Scale bars, 10 μ m.

10
11 **Fig. 4 | pSABER robustly amplifies fluorescent signals *in situ*.** **a**, Representative images of
12 DNA FISH targeting the mouse minor satellite repeat in EY.T4 mouse embryonic fibroblasts
13 visualized by SABER (left) or pSABER (right). Outlines of nuclei segmented using the DAPI
14 signal (yellow, dashed line) are overlaid on all images. Each image is presented at the indicated
15 high (top) and low (bottom) contrast settings to allow for visual comparisons between signals
16 occupying different portions of the 16-bit dynamic range (0–65535). **b**, Distributions of the peak
17 pixel intensity of each segmented puncta (see Methods). **c**, Normalized empirical cumulative
18 distributions of the peak pixel intensity of each segmented puncta showing fold-enhancement
19 over SABER, with vertical dashed lines corresponding to medians. A similar value of fold-
20 enhancement was obtained comparing means (25.1x enhancement, medians; 21.3x
21 enhancement, means). $n_{\text{SABER}} = 5,171$ puncta; $n_{\text{pSABER}} = 5,770$ puncta. Scale bars, 10 μ m.

22
23 **Fig. 5 | Exchange-pSABER enables highly amplified and multiplexed imaging.** **a**,
24 Schematic overview of Exchange-pSABER depicting sequential rounds of hybridization with an
25 HRP-oligo, development, displacement, and re-hybridization. **b**, 3 color Exchange-pSABER
26 experiment in EY.T4 mouse embryonic fibroblasts targeting the *Cbx5* mRNA (round 1, Cy5,
27 top), the 7SK RNA (round 2, Cy3, middle), and the ribosomal RNA internal transcribed spacer 1
28 (ITS1) region (round 3, fluorescein, bottom). **c**, A composite image of the 3-color Exchange-
29 pSABER experiment depicted in panel b taken using a SoRA CSU-W1 super-resolution
30 spinning disc microscope. **d**, Composite images of the 3-color Exchange-pSABER experiment
31 depicted in panel b taken using an automated slide-scanning microscope using 10x (left), 20x
32 (center), and 40x (right) air objectives. Images are maximum projections in Z (a–c) or single Z
33 slices (d). Scale bars, 10 μ m (a–c, fields of view), 20 μ m (d, insets), or 100 μ m (d, fields of view).

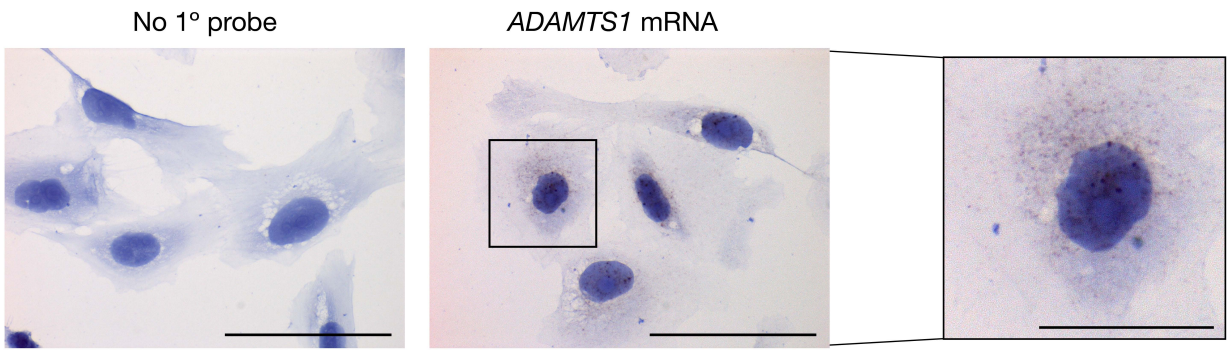
34
35 **Table 1 | Cost comparison of visualization reagents for SABER and pSABER.** The cost per
36 slide (center) and per imaging chamber slide well (right) are given for the key reagents needed
37 to visualize SABER and pSABER.

38
39 **Fig. S1 | Comparison of SABER and pSABER on a slide-scanning microscope.** **a**, SABER
40 (left) and pSABER (right) visualization of mouse major satellite DNA imaged using a 10x air
41 objective. **b**, SABER (left) and pSABER (right) visualization of mouse major satellite DNA
42 imaged using a 20x air objective. **c**, SABER (left) and pSABER (right) visualization of mouse
43 major satellite DNA imaged using a 10x air objective. Each image is presented at the indicated
44 high (top) and low (bottom) contrast settings to allow for visual comparisons between signals
45 occupying different portions of the 16-bit dynamic range (0–65535). Images are maximum
46 projections in Z. Scale bars, 20 μ m (insets) or 100 μ m (fields of view).

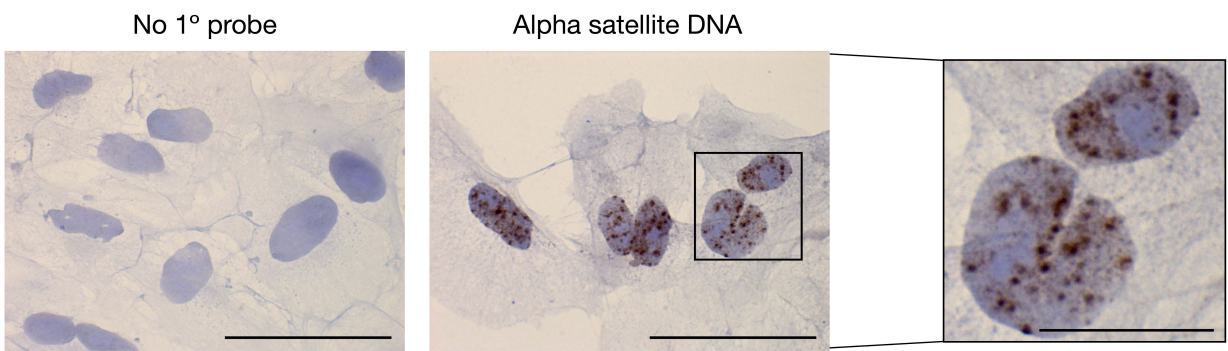


Figure 2 bioRxiv preprint doi: <https://doi.org/10.1101/2023.01.30.526264>; this version posted February 1, 2023. The copyright holder for this preprint (which was not certified by peer review) is the author/funder, who has granted bioRxiv a license to display the preprint in perpetuity. It is made available under aCC-BY-NC 4.0 International license.

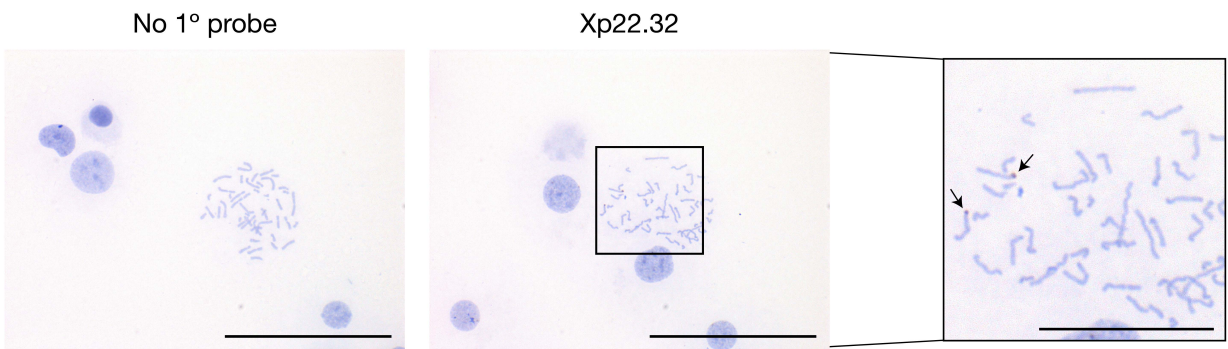
a



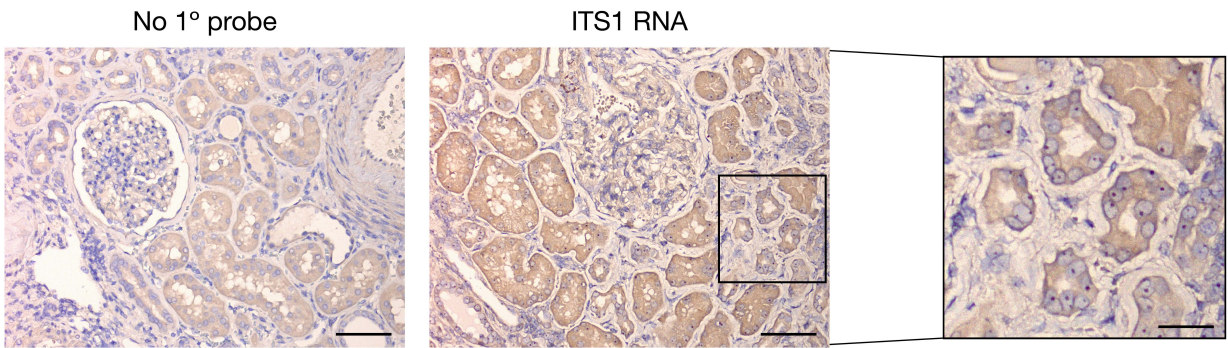
b



c



d



e

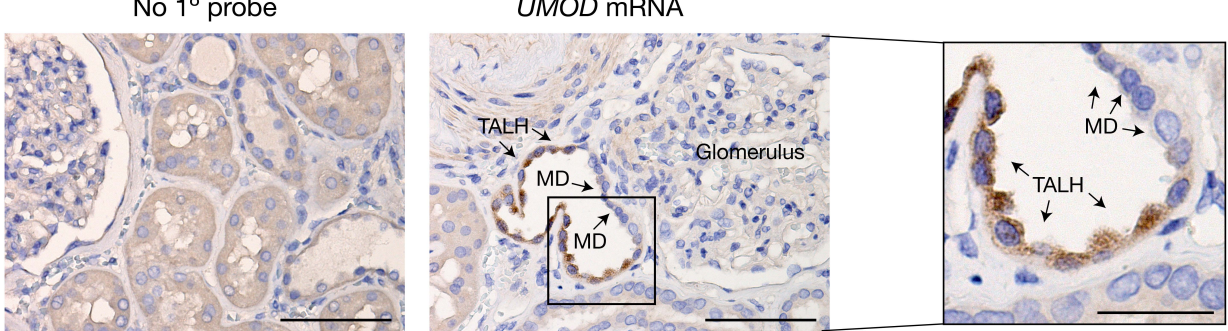
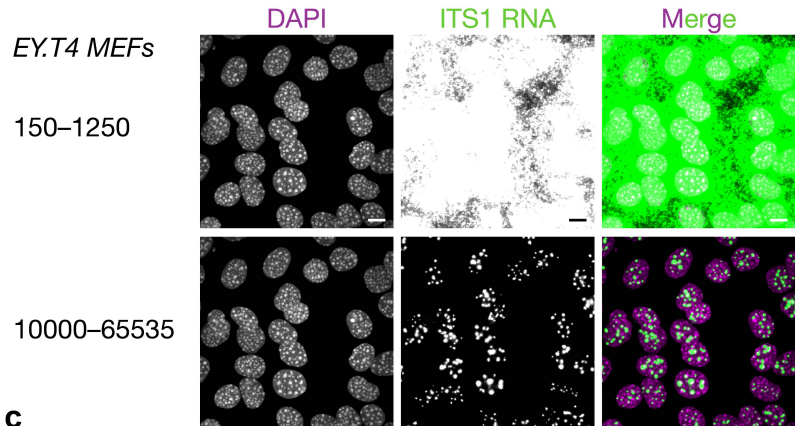
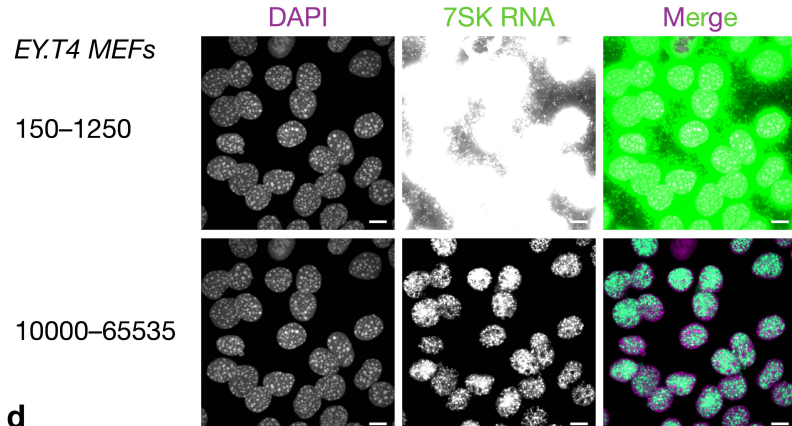


Figure 3 bioRxiv preprint doi: <https://doi.org/10.1101/2023.01.30.526264>; this version posted February 1, 2023. The copyright holder for this preprint (which was not certified by peer review) is the author/funder, who has granted bioRxiv a license to display the preprint in perpetuity. It is made available under aCC-BY-NC 4.0 International license.

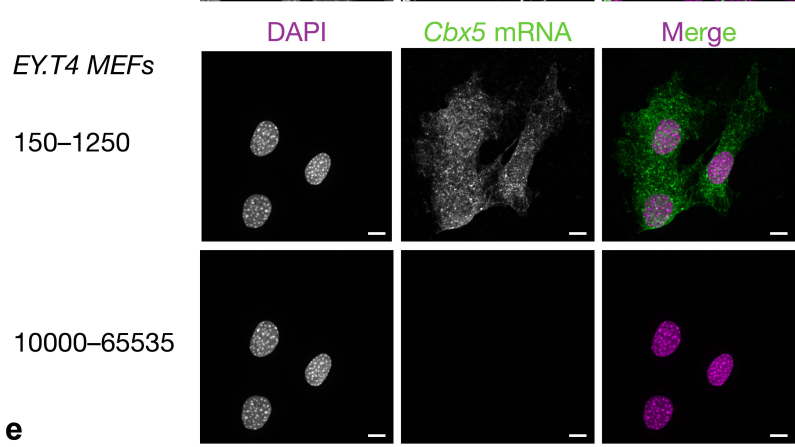
a



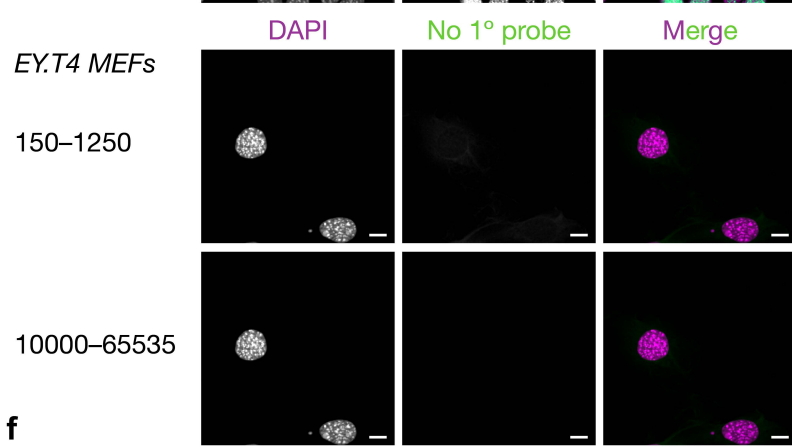
b



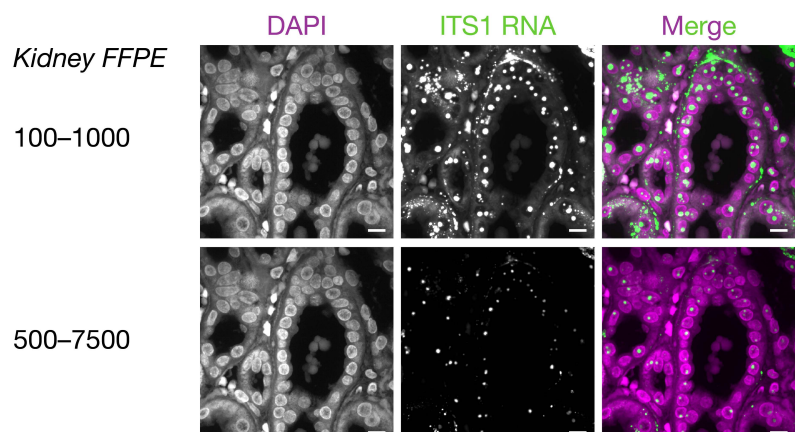
c



d



e



f

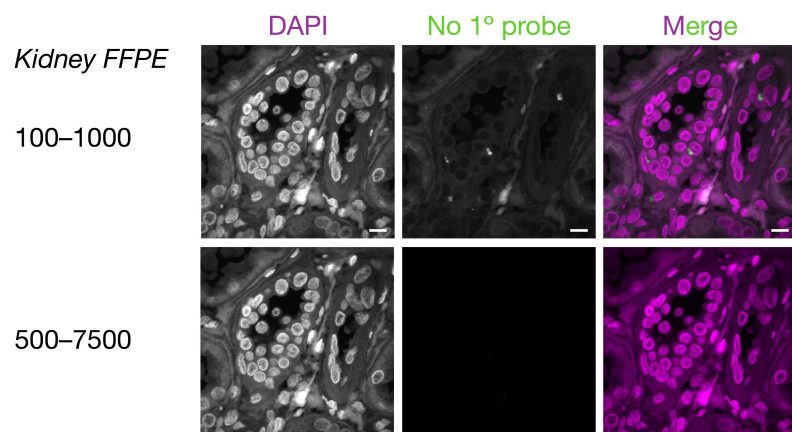
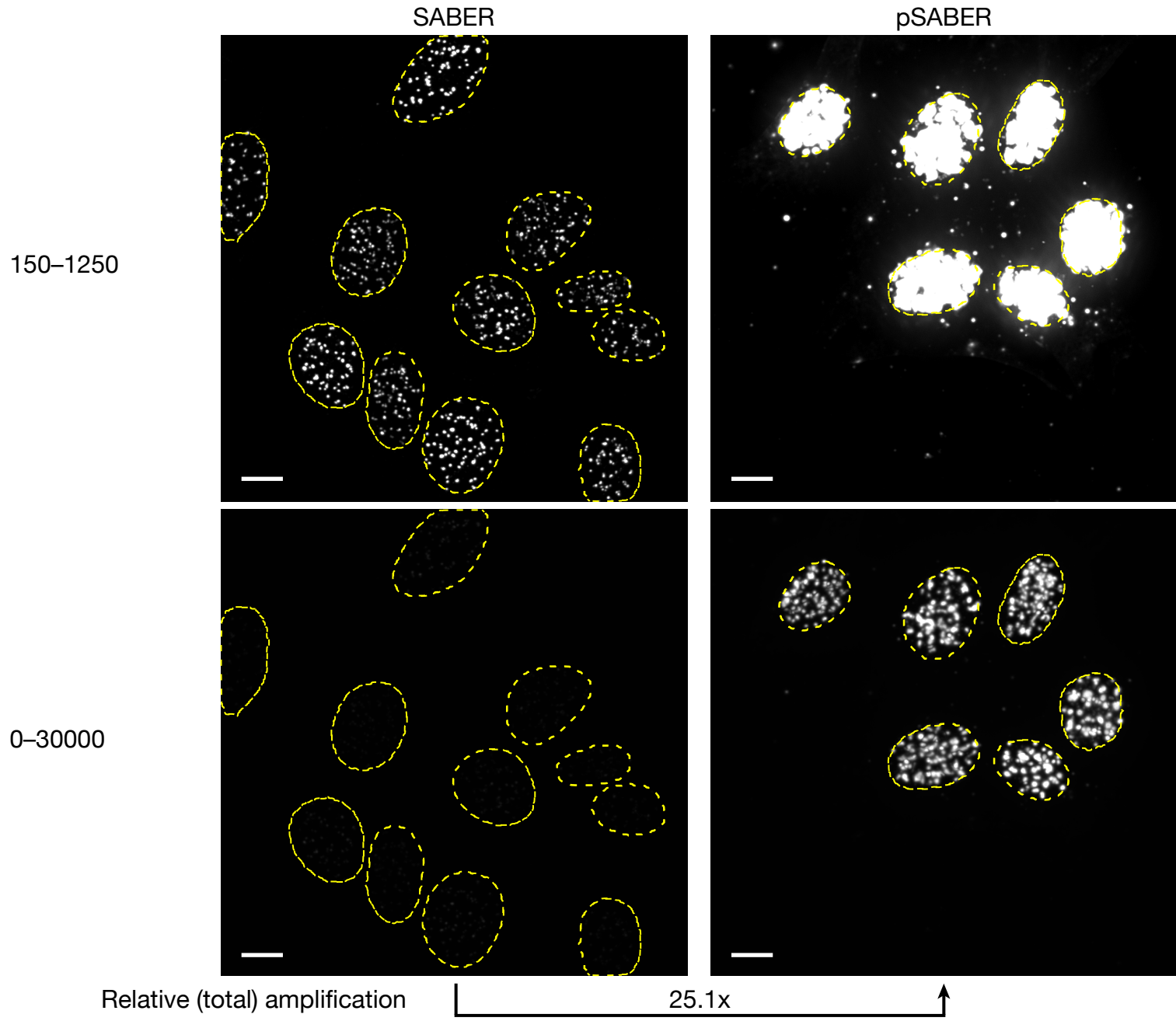
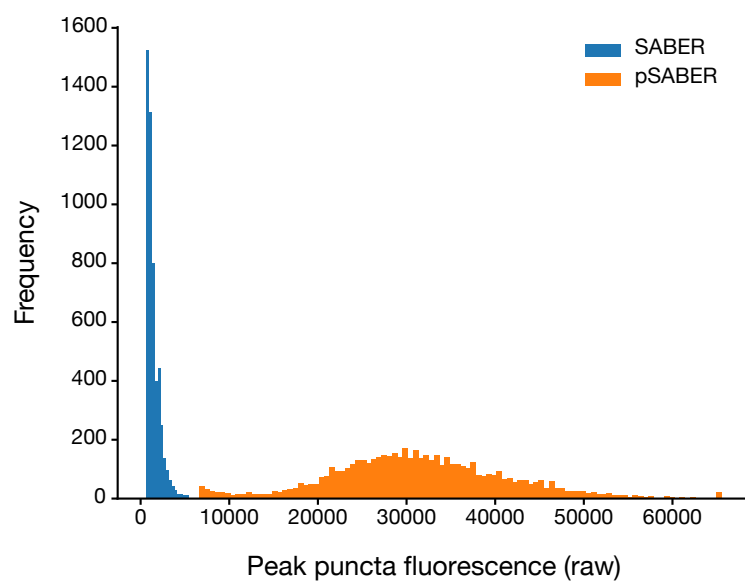


Figure 4 bioRxiv preprint doi: <https://doi.org/10.1101/2023.01.30.526264>; this version posted February 1, 2023. The copyright holder for this preprint (which was not certified by peer review) is the author/funder, who has granted bioRxiv a license to display the preprint in perpetuity. It is made available under aCC-BY-NC 4.0 International license.

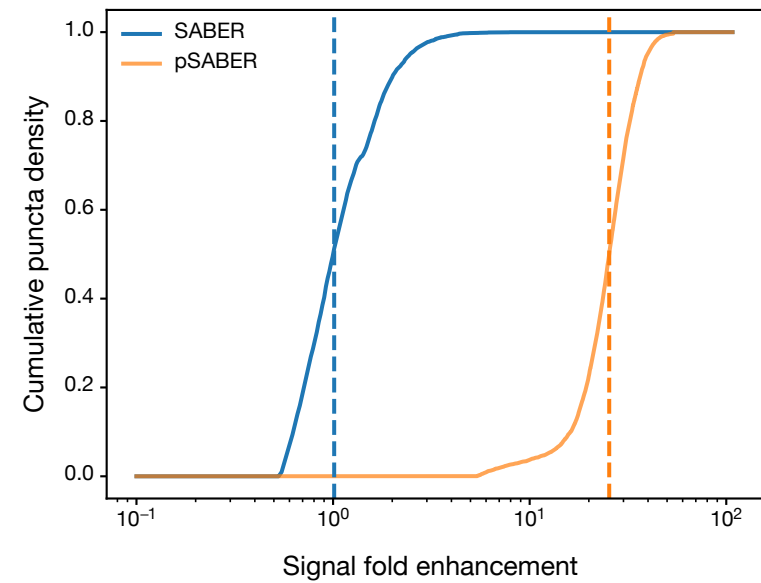
a

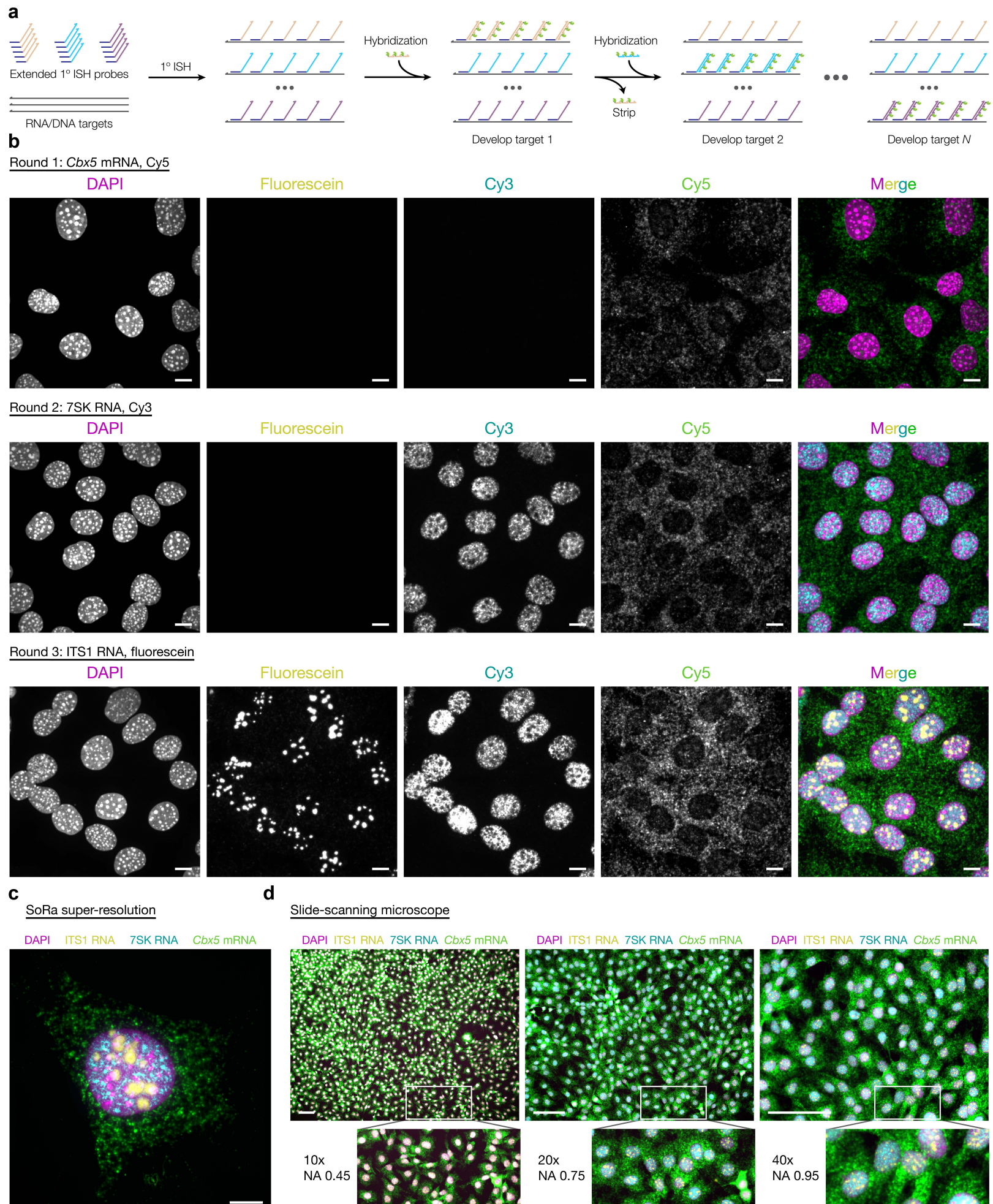


b



c





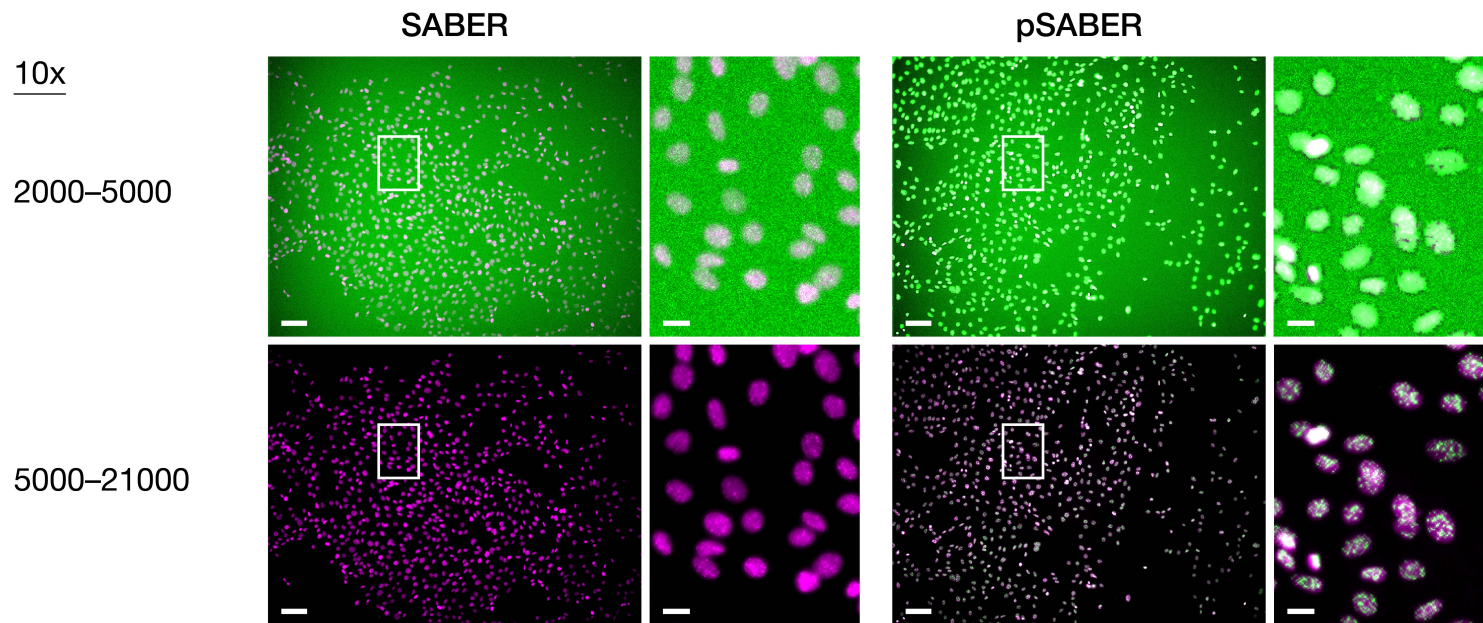
Reagent	Cost per slide (25 µl)	Cost per well (125 µl)
Fluor-oligo (SABER)	\$0.11	\$0.57
HRP oligo (pSABER)	\$0.44	\$2.22
Tyramide fluor (pSABER)	\$0.01	\$0.07

Table 1

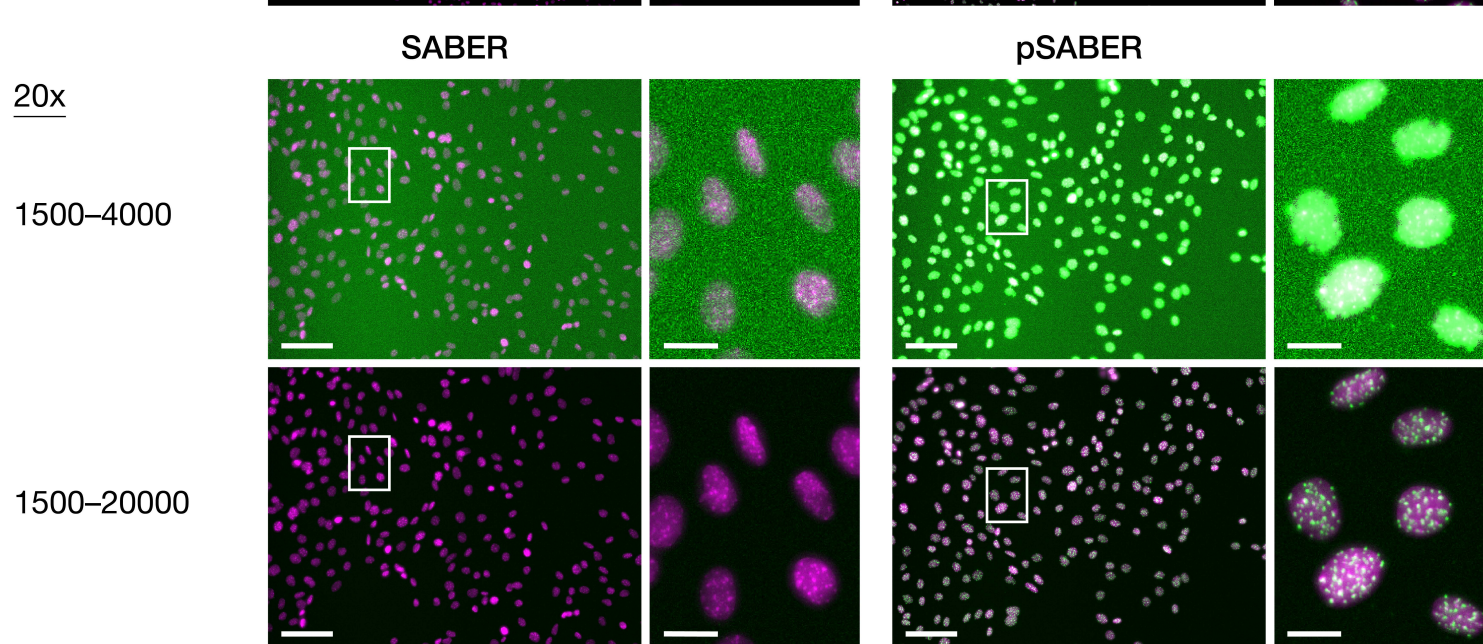
Figure S1

bioRxiv preprint doi: <https://doi.org/10.1101/2023.01.30.526264>; this version posted February 1, 2023. The copyright holder for this preprint (which was not certified by peer review) is the author/funder, who has granted bioRxiv a license to display the preprint in perpetuity. It is made available under aCC-BY-NC 4.0 International license.

a



b



c

